J. Physiol. (1980), **302**, *pp.* 535–547
With 6 text-figures
Printed in Great Britain

THE EFFECT OF CONTRAST ON THE NON-LINEAR RESPONSE OF THE Y CELL

BY R. M. SHAPLEY AND J. D. VICTOR
From the Rockefeller University, New York, N.Y. 10021, U.S.A.

(*Received 2 August 1979*)

SUMMARY

1. Second-order frequency responses were obtained from cat retinal ganglion cells of the Y type. The cells were stimulated by a spatial sine grating whose contrast was modulated in time by a sum of eight sinusoids.

2. Second-order frequency responses obtained at higher contrasts have a peak amplitude at higher input temporal frequency, and phase shifts, compared to their low-contrast counterparts.

3. This change in shape of the second-order frequency response is a departure from the prediction of the linear/static non-linear/linear sandwich model of the non-linear pathway in the cat retina. The departure is analysed by means of the hypothesis that the two filters of the sandwich model are parametric in contrast.

4. Most of the change in shape of the second-order frequency response with contrast is accounted for in terms of the sandwich model by changes in the transfer characteristics of the filter preceding the static non-linearity.

5. The effect of contrast on the second-order responses of Y cells is qualitatively similar in several ways to the effect of contrast on first-order responses. This suggests that the contrast gain control mechanism acts early in the retina, before linear and non-linear pathways have diverged.

INTRODUCTION

The Y cells of the cat retina may be distinguished physiologically by the presence of a non-linear excitatory mechanism in their receptive fields (Enroth-Cugell & Robson, 1966). Later investigations have suggested that the non-linear response of a Y cell is generated by an array of subunits scattered through the cell's receptive field (Hochstein & Shapley, 1976*a*, *b*). To a first approximation, the dynamics of this non-linear pathway are described by a model consisting of a linear filter representing the pooling of light by each subunit, followed by a static non-linearity similar to a rectifier, followed by a second linear filter representing the pooling of the subunit responses (Victor, Shapley & Knight, 1977; Victor & Shapley, 1979*b*).

However, a Y cell's non-linear responses, as reflected by its second-order frequency responses (or kernels), depart somewhat from the simple linear/static non-linear/linear 'sandwich' model, especially in the dependence on contrast. In this report, the sandwich model is elaborated to account for the second-order contrast effect by allowing the two 'linear' filters of the sandwich model to have transfer properties parametric in contrast.

0022-3751/80/8250-0426 $07.50

The frequency-response method we have used has the advantage that the second-order frequency responses of some model systems have simple algebraic forms. Using this analytical tool, we have been able to dissect the effect of contrast on the second-order frequency response into its separate effects on the first and second linear filters of the sandwich model. The analysis suggests that contrast-dependent changes in the first linear filter are primarily responsible for the departure from the simple sandwich model.

The effect of contrast on the second-order response of Y cells is qualitatively similar in many ways to its effect on the first-order responses of both X and Y cells (Shapley & Victor, 1978). This similarity, and the fact that we can infer that the major effect of contrast is on the pre-filter in the sandwich model, suggest that the contrast gain control acts before the linear and non-linear pathways diverge in the retina.

METHODS

Our methods of visual stimulation, recording, and data analysis have been described in detail previously (Hochstein & Shapley, 1976*a*); we outline them briefly here.

Physiological recording. Recordings were made from optic tract fibres of adult cats anaesthetized with urethane. The cat's e.k.g., e.e.g., blood pressure, core temperature, end-expiratory CO_2, and optics were monitored and maintained in the physiological range. The cats were fitted with a +2D contact lens which had a 3 mm artificial pupil. Action potentials, recorded extracellularly with tungsten-in-glass micro-electrodes (Levick, 1972), triggered a discriminator circuit which sent shaped pulses to a PDP 11/20 computer, which recorded their arrival time to within 0·1 msec.

Visual stimuli. Visual stimulation was accomplished with a cathode ray tube at a distance of 57 cm. The area of display was 20 cm × 20 cm which spanned a visual angle of 20° × 20°. The mean luminance of the cathode ray tube was 10–20 cd/m^2. Spatial patterns were produced on it with a specialized set of circuits (Shapley & Rossetto, 1976) to control the X, Y, and Z inputs. The spatial patterns used in these experiments were standing sine gratings (oriented vertically) of arbitrary spatial phase and spatial frequency. The contrast of the pattern was modulated in time by a control signal from the 11/20 computer. A control voltage of zero produced a uniform display at the mean luminance; when the control voltage passed through zero the contrast reversed.

Second-order frequency responses. The temporal modulation signal was a sum of eight nearly incommensurate sinusoids. The frequencies of the sinusoidal components were typically: 0·214 Hz, 0·458 Hz, 0·946 Hz, 1·923 Hz, 3·876 Hz, 7·782 Hz, 15·594 Hz and 31·219 Hz. These frequencies are related as harmonics of a common fundamental frequency; the jth frequency is the 2^{j+2}-1 harmonic of the base frequency 0·0305 Hz. The reason for the choice of this set of input frequencies is that first-order and second-order combination frequencies of this set are all distinct output frequencies. The neural responses were Fourier-analysed at each of the input frequencies, as well as each of the second-order frequencies (sums and differences of the input frequencies). This report is concerned only with second-order components of the responses of the Y cell. The Fourier component at the sum of two input frequencies f_i+f_j yielded an experimental estimate of the second order frequency response $K_2(f_i, f_j)$. The Fourier component at the difference of two input frequencies f_i-f_j yielded an experimental estimate of $K_2(f_i, -f_j)$. The second-order frequency response $K_2(F_1, F_2)$ is thought of as a continuous function of two frequencies; an interpolation procedure was used to estimate the values of the second-order responses at points not on the lattice of input frequency pairs. The resulting function of two variables was plotted as a surface (e.g. Fig. 2 below) whose height at any point (F_1, F_2) represents the amplitude of $K_2(F_1, F_2)$. For further discussion, see Victor & Knight (1979) and Victor & Shapley (1979*a*, *b*).

Experimental protocol. After isolation of a single optic tract fibre, the receptive field was mapped on a tangent screen. The receptive field centre was positioned in the centre of the

cathode ray tube display with a mirror, and the unit was classified as X or Y by a modified null test (Hochstein & Shapley, 1976*a*). Only Y cells were used in this study and off-centre cells were used only if their maintained discharge was substantial. The temporal modulation signal was placed under computer control to study dynamics of the response to as many spatial frequencies, spatial phases, and contrasts as time permitted. For each spatial pattern, several contrast levels were presented in interleaved runs. The peak contrast produced by each sinusoidal component was typically 0·0125, 0·025, 0·05 and 0·10 in successive runs (Contrast = $(I_{max}-I_{min})/(I_{max}+I_{min})$). All frequency responses (kernels) were calculated from an average over different relative phases of the input sinusoids, to remove fourth and sixth order components (Victor & Knight, 1979). The phase averaging also reduced the noise in the measurements: the typical standard error was 1–2 impulses/sec.

The cell population in this study consisted of ninety-three Y cells (sixty-seven on-centre, twenty-six off-centre).

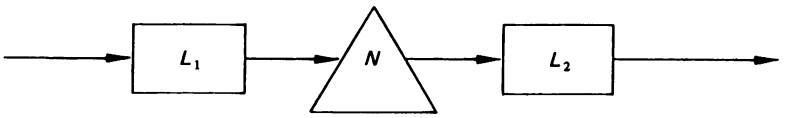

Fig. 1. This is a diagram of the linear/non-linear/linear sandwich model which can be used to understand the major qualitative features of second-order frequency responses. The transducer N is hypothesized to be the only non-linear stage in the retinal pathway leading to the Y cell. L_1 is the spatio-temporal filter (characteristic of each subunit) which precedes the non-linearity N. L_2 is the filter which represents the process of summing the subunit outputs after the non-linearity.

RESULTS

Second-order frequency responses and the sandwich model

A simple dynamical model, consisting of a linear filter, L_1, followed by a static non-linearity, N, followed by a second linear filter, L_2 has been advanced as a good description of the non-linear pathway of the Y cell (Victor & Shapley, 1979*b*). A block diagram of such a model is shown in Fig. 1. The second-order frequency response of such a network has the functional form

$$K_2(f_1, f_2) = b(N; C)\tilde{L}_1(f_1)\tilde{L}_1(f_2)\tilde{L}_2(f_1+f_2) \quad (1)$$

where $\tilde{L}_1$ and $\tilde{L}_2$ are the transfer functions of L_1 and L_2. The constant $b(N, C)$ is real; it depends on the input contrast C, the filter L_1 and the shape of the static non-linearity N (Spekreijse, Estevez & Reits, 1977; Victor & Knight, 1979).

The major qualitative features of the second-order frequency responses of a Y cell shown in Fig. 2 can be understood in terms of the linear/non-linear/linear sandwich model (Fig. 1 and eqn. (1)). For instance, there is always one major peak of the amplitude surface in the sum quadrant (F_1 and F_2 both positive) and another peak at about the same input frequency in the difference frequency quadrant (F_2 positive, F_1 negative). These peaks mainly reflect the characteristics of the bandpass filter before the non-linearity, L_1. If there were no post-filter L_2, then for a given pair of input frequencies the sandwich model would produce identical amplitudes of the sum and difference frequency components. Whatever asymmetry there is between sum and difference frequency quadrants is due to the post-filter L_2. In fact, one can see from the form of eqn. (1) that L_1 acts on the *input frequencies* while L_2 acts on the *harmonic*

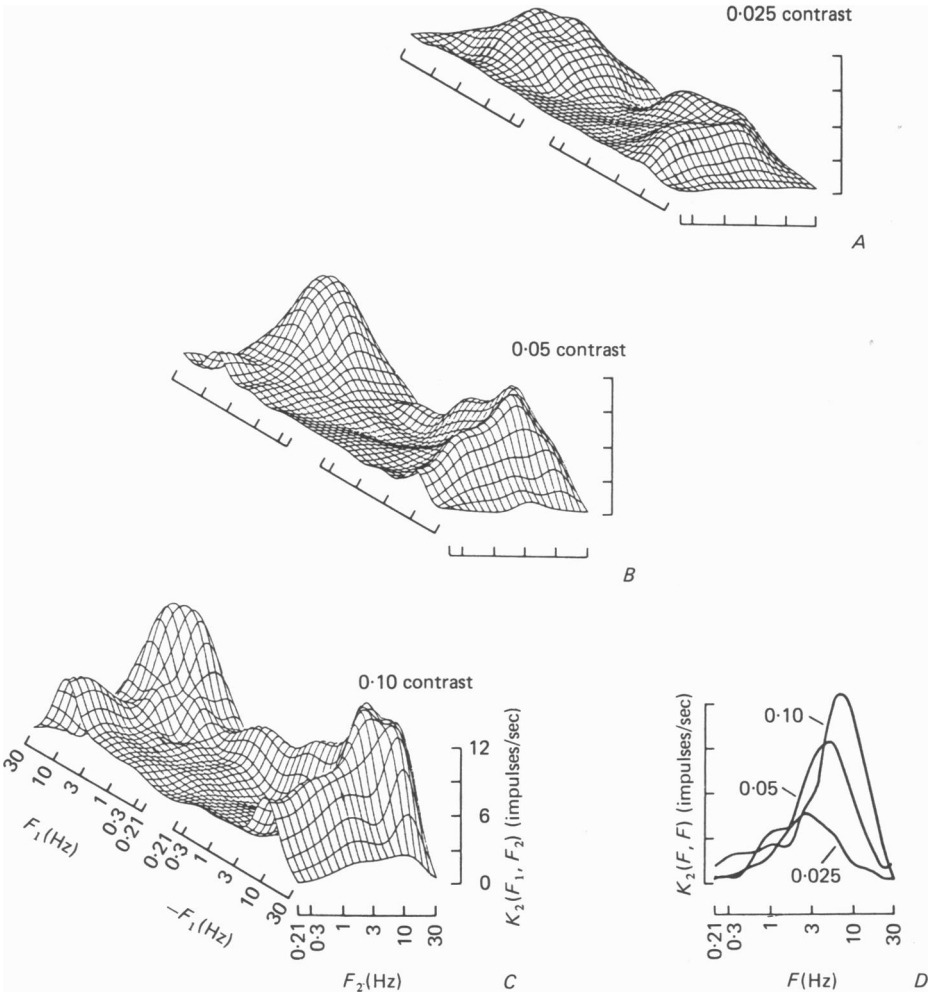

Fig. 2. Amplitudes of the second-order frequency kernel as a function of contrast in an on-centre Y cell. Second-order kernels were obtained at three contrast levels: 0·025/sinusoid (*A*), 0·05/sinusoid (*B*), and 0·1/sinusoid (*C*). The spatial pattern was a 0·6 c/deg grating, which produced no first-order responses in any spatial phase. The response shifts to higher temporal frequencies with increased contrast. In this and all other data presented here, luminance was 20 cd/m². *D* shows the amplitudes of the pure second-harmonic components $K_2(f_i, f_i)$. Unit 13/10.

and intermodulation frequencies. Thus, characteristics of the second-order frequency responses which are tied to the input frequencies reflect L_1 and characteristics which depend on output frequency reflect L_2.

The simple sandwich model predicts that the second-order frequency responses should grow with contrast but should neither change shape nor undergo any phase shifts. This follows from eqn. (1) where the only dependence on contrast is contained in the real valued scale factor $b(N; C)$. The static non-linearity may cause $b(N; C)$ to be a non-linear function of contrast but that will not affect either the relative amplitudes of $K_2(F_1, F_2)$ or the phases of the second-order responses.

We found that the second-order frequency responses of Y cells showed an unequivocal dependence on contrast in contradiction to the simple sandwich model. This was true for spatial gratings of all spatial frequencies. An example of the contrast dependence of the second-order frequency response in a typical Y cell is shown in Fig. 2.

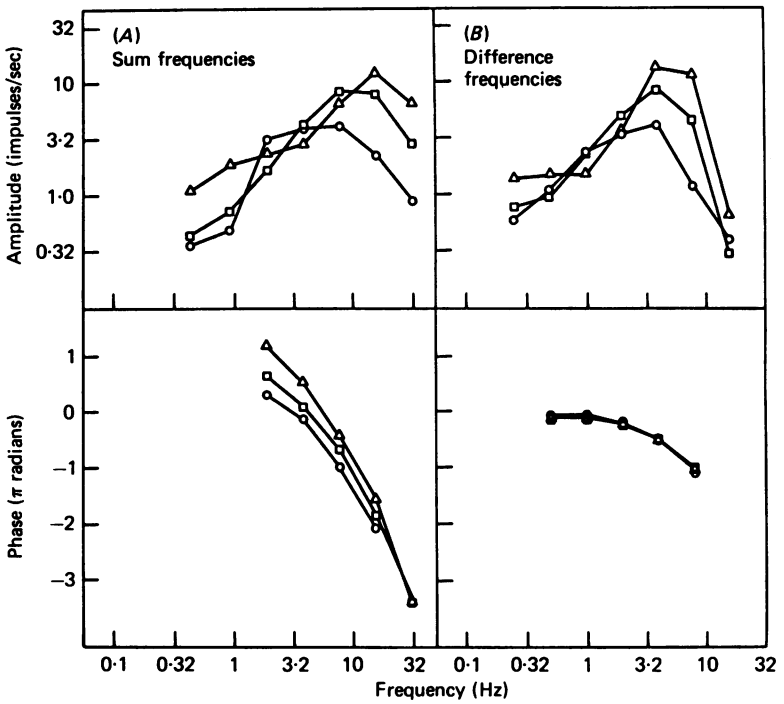

Fig. 3. Behaviour of selected amplitude and phase values of the second-order frequency kernel as a function of contrast, measured in the experiment of Fig. 2. The three levels of contrast are indicated by the symbols: ○, 0·025/sinusoid; □, 0·05/sinusoid and △, 0·1/sinusoid. In *A*, amplitudes and phases of $K_2(f_i, f_i)$ are plotted as a function of the output frequency $2f_i$. In *B*, amplitude and phases of $K_2(f_{i+1}, -f_i)$ are plotted as a function of the output frequency, $f_{i+1} - f_i$. Phases are indicated only for data points at which the amplitude was significantly different from zero. The substantial phase shift for the sum frequencies (*A*), contrasted with the negligible phase shift for the difference frequencies (*B*), indicates that the phase shift is the result of a process before the generation of the sum and difference frequencies. Unit 13/10.

The positions of the peak responses shifted to higher temporal frequencies as input contrast increased, as one can see by comparing Fig. 2*A* with 2*B* and *C*. At a contrast of 0·025 per sinusoid (Fig. 2*A*), the second-order frequency response had a peak amplitude of approximately 4 impulses/sec at an input frequency of 3 Hz, along the line of pure second harmonics (where $F_1 = F_2$). In the difference region ($K_2(-F_1, F_2)$), there was a peak amplitude of a similar height at an input frequency of about 5 Hz. When the input contrast was doubled to a level of 0·05 per sinusoid (Fig. 2*B*), the peak amplitude, which had a value of 8 impulses/sec, occurred at a higher input frequency: 6 Hz along the line of pure second harmonics. The peak in the difference region also shifted up to an input frequency of approximately 7 Hz. At the still

higher input contrast level of 0·10 per sinusoid, the second-order frequency response showed further changes in the same direction (Fig. 2*C*). Despite peak amplitudes of over 12 impulses/sec, there was almost no second-order response when either one of the two input frequencies was less than 2 Hz. The input temporal frequencies which produced the greatest second-order responses were even higher than before. The greatest amplitude measured in the sum region was at an input frequency of 8 Hz; in the difference region, there was a broad plateau extending to approximately 12 Hz. These data are typical for the entire population of Y cells we studied.

Fig. 2*D* shows a subset of the second-order frequency response, the second harmonic frequency response $K_2(F_1, F_1)$. The second harmonics lie on the diagonal line of unit slope ($F_1 = F_2$) which passes through the origin in the sum quadrants of Figs. 2*A–C*. The amplitudes of the second harmonics show the same qualitative dependence on contrast as does the entire second-order frequency response: a shift of the peak amplitude to higher temporal frequency at higher contrast.

The contrast dependence of the second-order responses of Fig. 2 were examined in another way in Fig. 3, in order to ascertain the dependence of the *phase* of the responses on contrast. Here we have plotted amplitudes and phases of the components of the second-order frequency responses that lie either on the pure second harmonic diagonal in the sum frequency quadrant (Fig. 3*A*) or just off the line of zero output frequency in the difference frequency quadrant (Fig. 3*B*). In each case, the abscissa is the *output frequency* of the measured second-order response. (Note that in Fig. 2 the co-ordinates F_1 and F_2 refer to the *input* frequencies.) In Fig. 3*A* we have plotted the amplitudes and phases of the second harmonic components; these are the values of the second-order frequency response for which the two input frequencies which are added to produce the second-order combination frequency are identical. Thus, the second harmonics are a subset of the second-order frequency responses and are denoted $K_2(f_i, f_i)$. These values are derived from the Fourier component of the response at the pure second harmonic $2f_i$ of the ith input frequency, f_i. In Fig. 3*B*, we have plotted the amplitudes and phases of $K_2(f_i, -f_{i-1})$. The amplitude curves shown in Fig. 3 are diagonal slices through the surface of the second-order frequency kernel as shown graphically in Fig. 2; the corresponding phase curves yield additional information absent from the amplitude plots.

The dependence of amplitude on contrast is the same for the two sets of curves, but the phase dependence is qualitatively different. Both sets of amplitude curves show a shift of the peak response to higher temporal frequencies as input contrast increases, as mentioned above. It is also clear that the responses to high temporal frequencies increase more rapidly with contrast than do the responses to lower temporal frequencies. However, the dependence of phase on input contrast is not the same for sum frequencies and difference frequencies. The phases of the responses to sum frequencies advance rapidly with contrast, as can be seen in the lower half of Fig. 3*A*. As may be seen from Fig. 3*B*, the phases of the responses of difference frequencies do not vary appreciably with contrast. That is, the contrast dependence of the phase of a second-order response is a function not merely of its output frequency, but also whether this particular second-order combination frequency is a sum frequency or a difference frequency. The magnitude of the phase shifts in this unit were typical for our population of cells. The phase of $K_2(8, 8)$ usually advanced

by 0·4–0·6π radians (72–108°) as contrast varied from 0·0125/sinusoid to 0·10/sinusoid. This is about twice the size of the phase shift with contrast we have reported for the first-order response near 8 Hz (Shapley & Victor, 1978).

Increasing the contrast produced shifts of the peak second-order amplitude to higher temporal frequency and also phase advances. These results were reminiscent of our earlier observations on the effect of contrast on first-order responses of X and Y cells. Our main aim was to produce a successor to the simple sandwich model which

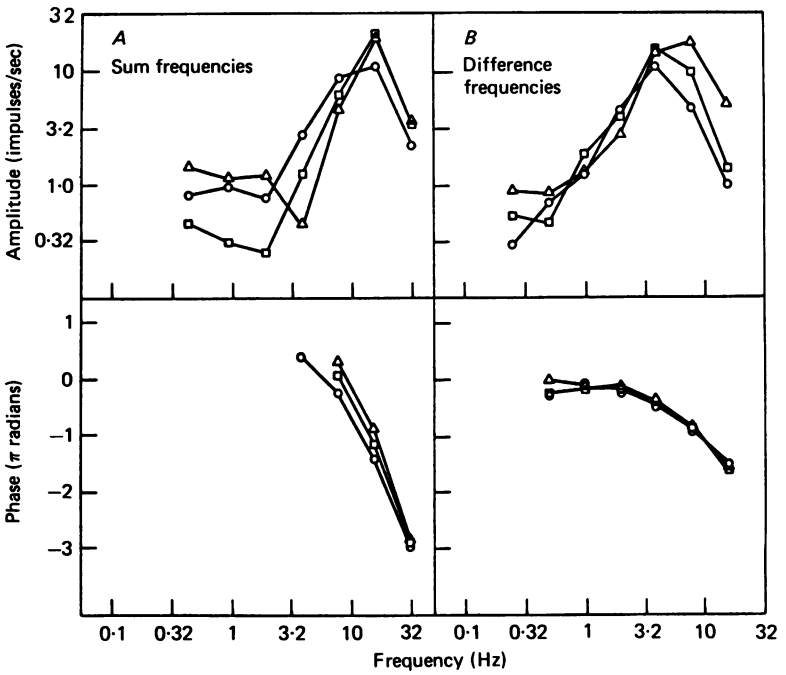

Fig. 4. Behaviour of selected amplitude and phase values of the second-order frequency kernel as a function of contrast for a low spatial frequency grating in the 'peak' position. Data are displayed as in Fig. 3. The unit was the on-centre Y cell of Fig. 2, and the spatial pattern was a 0·1 c/d grating, positioned $\frac{1}{4}$ of a period away from the 'null' position so that maximal first-order responses were obtained. Peak first-order responses were: 24, 40, and 42 impulses/sec at contrasts of 0·025, 0·05 and 0·1/sinusoid respectively. Despite the presence of a large linear response, the data are virtually identical to those of Fig. 5. Unit 13/14.

could account for these second-order contrast effects. Before we could do this we had to determine whether the second-order contrast effect shared one other important property with the first-order contrast effect, namely invariance with spatial phase of the grating stimulus.

Parametric dependence on contrast: independence of spatial phase. In the data presented so far, we have not attempted to distinguish between the retinal contrast and the size of the ganglion cell's response as factors that alter the transfer properties in ganglion cells. However, retinal contrast and the size of a ganglion cell's *linear* response may be varied independently by varying the spatial phase of a sinusoidal grating. We have found that the second-order frequency response of Y cells is

independent of spatial phase, even when the spatial frequency of the stimulus is low enough to produce a large linear response (Victor & Shapley, 1979*b*). Thus one would certainly expect that the change in shape of the second-order kernel due to contrast should also be independent of spatial phase. That this is true is shown by the data of Figs. 4 and 5. Here, amplitudes and phases of the second-order frequency response obtained from an on-centre Y cell are plotted as a function of output temporal frequency. Measurements were made at three input contrasts: 0·25, 0·05, 0·10 per sinusoid. The stimulus was a 0·1 c/deg grating.

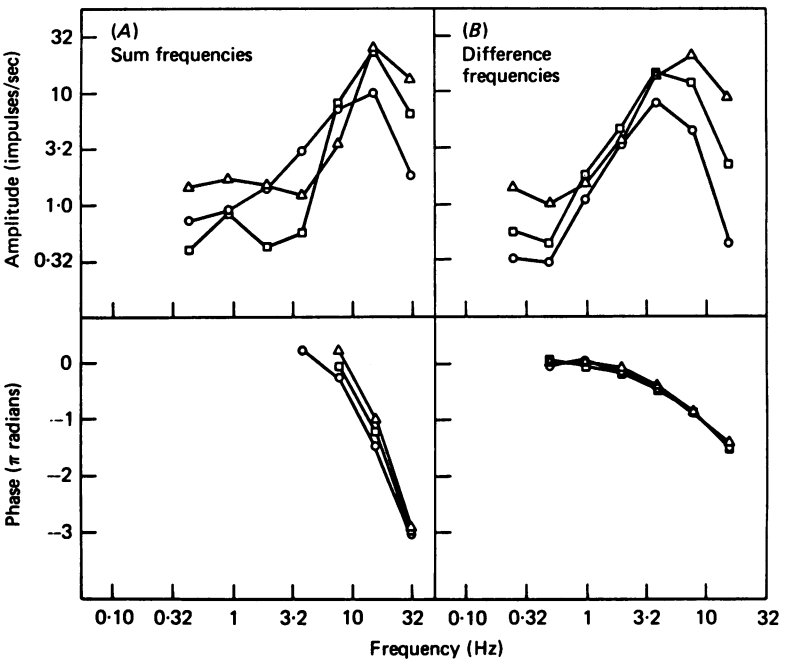

Fig. 5. Behaviour of selected amplitudes and phase values of the second-order frequency kernel as a function of contrast for a low spatial frequency grating in the 'null' position. Data are displayed as in Fig. 3. The unit was an on-centre Y cell, and the spatial pattern was a 0·1 c/d grating positioned so that the greatest first-order response at the highest contrast was 2 impulses/sec. Unit 13/14.

Two spatial phases were used. One (Fig. 4) was the spatial phase for the maximal first-order response ('the peak'). The other (Fig. 5) was the position at which the first-order responses were close to zero (the null position for the first-order responses, here abbreviated as 'the null position'). These spatial phases were separated by 90° as they always are in X and Y cells (Hochstein & Shapley, 1976*a*; Victor & Shapley, 1979*a*, *b*).

Although the first-order response amplitudes varied from a maximum of 42 impulses/sec at the 'peak' position (Fig. 4) to 2 impulses/sec or less at the 'null' position (Fig. 5), the amplitudes and phases of the second-order responses show virtually identical contrast dependence at the two spatial phases. It is also clear that the behaviour of the second harmonic phase shifts differ strikingly from the behaviour of the difference-frequency phase shifts and this behaviour is independent of spatial

phase. Thus, the effect of contrast on the second-order responses is independent of the spatial phase of the grating stimulus.

The elaborated sandwich model. There are many ways of elaborating the linear/non-linear/linear sandwich model to account for the effects of contrast. The generalization that we choose to pursue here is a logical extension of the model introduced to explain the variation of the first-order responses of X and Y cells with contrast (Shapley & Victor, 1978). The block diagram of the elaborated sandwich model is

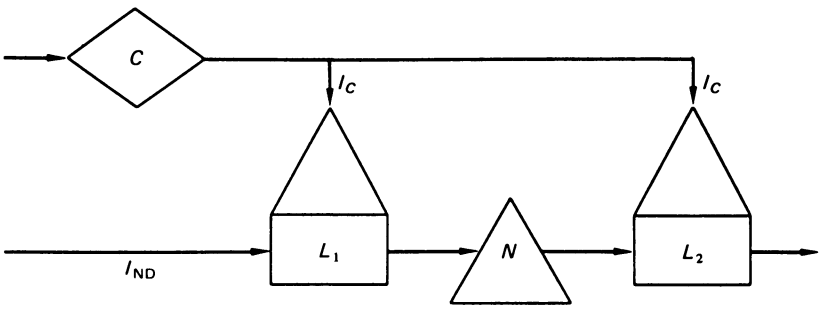

Fig. 6. A model for the effect of contrast on the non-linear pathway of the Y cell. The direct input to the non-linear pathway, I_{ND}, is transformed in succession by the filter L_1, the static non-linearity N, and the second filter, L_2. A signal I_C indicating total contrast over the nearby regions of retina is generated by the network C, and forms a second input to L_1 and L_2. For constant values of I_C, L_1 and L_2 are assumed to be linear, and the response to I_{ND} is that of a simple linear/static non-linear/linear model. The action of I_C on L_1 and L_2 must be complex, and includes a phase advance at high temporal frequencies and a relative suppression of low temporal frequencies.

shown in Fig. 6. We postulate a neural signal I_C representing the average amount of contrast over a fairly wide region of retina. We call the direct input to the non-linear network of the Y cell I_{ND}. The contrast signal I_C modulates the transfer properties of L_1 and L_2 (Fig. 6). For constant values of I_C, both L_1 and L_2 are linear, and the response of the Y cell non-linear pathway to I_{ND} has the form of eqn. (1). That is,

$$K_2(f_1, f_2; C) = b(N; C)\tilde{L}_1(f_1; I_C)\tilde{L}_1(f_2; I_C)\tilde{L}_2(f_1+f_2; I_C), \tag{2}$$

where $K_2(f_1, f_2; C)$ is the second-order frequency response obtained at the contrast level C, and $\tilde{L}_1(f_1; C)$ and $\tilde{L}_2(f_2; C)$ are the transfer functions of L_1 and L_2 when the contrast signal I_C has a level C.

Rigorously, this formulation assumes that the signal I_C is a constant in time, which implies that the network C which measures I_C has an integrator with an indefinitely long time constant as its final stage. If the signal I_C is *not* steady, it is necessary to specify the mode of interaction between I_C and the filters L_1 and L_2. Clearly, if the variations of I_C with time are small and slow in comparison to the time constants of L_1 and L_2, eqn. (2) remains valid with interpretation of $\tilde{L}_1(f; I_C)$ and $\tilde{L}_2(f; I_C)$ as the transfer functions of the filters L_1 and L_2 if I_C were constant at its average value. Furthermore, numerical simulations show that the functional form (2) remains a good approximation, even when the time course of fluctuations of I_C are comparable to the time constants of the filters L_1 and L_2 (Victor, 1979).

The model described by eqn. (2) has many more free parameters than its simple sandwich counterpart: the functional forms of $\tilde{L}_1$ and $\tilde{L}_2$, as well as their dependence

on I_C are unspecified. Thus, it is difficult to obtain a criterion of the 'goodness of fit' of eqn. (2) to the data.

Nevertheless, the contrast-dependent sandwich model is useful because it allows one to separate the effect of contrast on the filter preceding the non-linearity from its effect on the filter following the non-linearity. For this purpose, it suffices to consider only the phase difference, $\Delta\phi(f_1, f_2)$, between the second-order frequency responses measured at two contrasts C and C':

$$\Delta\phi(f_1, f_2) = \Delta\phi_1(f_1) + \Delta\phi_1(f_2) + \Delta\phi_2(f_1 + f_2) \tag{3}$$

$\Delta\phi_1(f)$ and $\Delta\phi_2(f)$ denote the phase changes in $\tilde{L}_1$ and $\tilde{L}_2$ as the contrast is changed from C to C'. The term $b(N; C)$ in eqn. (2) is real-valued, and thus does not affect the phase of the response.

Suppose that the linear filter L_1 preceding N is insensitive to contrast. Then, $\Delta\phi_1 = 0$, and eqn. (3) would predict that

$$\Delta\phi(f_1, f_2) = \Delta\phi_2(f_1 + f_2),$$

which states that the phase shift with contrast of a component in the second-order response depends only on its output frequency. This prediction stands in contradiction to what we have observed. In Figs. 3–5, the phase advances of second-order components $K_2(f_j, f_j)$ are substantial (up to $0{\cdot}5\pi$ radians), while the phase advances of the second-order components $K_2(f_{j+2}, -f_{j+1})$ are typically less than $0{\cdot}1\pi$ radians at all these high frequencies. However, the output frequencies of these two second-order components, $2f_j$ and $f_{j+2} - f_{j+1}$, are nearly identical (they differ by approximately 0·03 Hz).

Thus, we are led to the conclusion that at least some of the effect of contrast is exerted in L_1, before generation of the non-linear response. Now let us suppose that *all* of the parametric dependence on contrast is accounted for by L_1. Then $\Delta\phi_2 = 0$, and eqn. (3) predicts that

$$\Delta\phi(f_1, f_2) = \Delta\phi_1(f_1) + \Delta\phi_1(f_2) \tag{4}$$

$$\Delta\phi(f_1, f_1) = 2\Delta\phi_1(f_1). \tag{4a}$$

Since $\tilde{L}_1(f)$ is the Fourier transform of a real function, $\Delta\phi_1(-f) = -\Delta\phi_1(f)$. Therefore, we can use eqns. (4) and (4*a*) to derive

$$\Delta\phi(f_1, \pm f_2) = \tfrac{1}{2}(\Delta\phi(f_1, f_1) \pm \Delta\phi(f_2, f_2)). \tag{5}$$

This equation predicts the phase shift of each component of the second-order frequency response from the phase shifts of the pure second harmonic responses alone. In particular, it predicts that the phase shift at a difference frequency $f_1 - f_2$ should be zero if, and only if, the phase shifts at the corresponding pure second harmonic frequencies, $2f_1$ and $2f_2$, are identical. This is well supported by the data in Figs. 4 and 5. But in Fig. 3 the phase shift $\Delta\phi(f, f)$ is a steadily decreasing function of output frequency. In this instance, eqn. (5) predicts that $\Delta\phi(f_{j+1}, -f_j)$ should be negative. The fact that $\Delta\phi(f_{j+1}, -f_j)$ is approximately zero therefore suggests the presence in this case of a slight phase advance contributed by L_2.

In summary, this analysis of the effect of contrast on the second-order frequency response shows that most of the effect occurs only before the static non-linearity of

the sandwich model, but in some units an additional effect on the second filter L_2 can be demonstrated.

We have also performed a more complete analysis which involved fitting the log-amplitudes and phases of the second order frequency responses with polynomials and determining the effects of contrast. This more complete analysis supports the main conclusion above; contrast mainly affects the pre-filter L_1.

DISCUSSION

In searching for a suitable model that is complex enough to explain the contrast effect, yet simple enough to analyse, we have been guided by the same considerations that we used in constructing the two-input model for the first-order frequency response (Shapley & Victor, 1978). Because eqn. (1) provides a good fit to the second-order frequency response at a single contrast level (Victor *et al.* 1977), we would like to elaborate on the sandwich model, rather than abandon it entirely. One possible such extension is a model consisting of two parallel sandwich subsystems. However, without an *a priori* idea of what the two parallel paths represent it is very difficult to make any non-trivial statements based on the experimental data about the nature of the linear and non-linear components. Another possible extension is the 'club sandwich' model, in which L_2 is followed by a second static non-linearity N' which in turn is followed by a third linear filter L_3. However, the 'club sandwich' model is difficult to analyse in the large-signal regime. The model we have chosen, the sandwich model parametric in contrast (Fig. 6), has the distinct advantage that it is susceptible to analysis. Also, this model allows direct comparison with the effect of contrast on the first-order response.

Comparison with the effect on the first-order frequency responses

There are many similarities between the effect of contrast on the second-order responses of Y cells and its effect on the first-order responses of both X and Y cells (Shapley & Victor, 1978). In both cases, the shapes of the amplitude functions are independent of spatial phase and hence independent of the size of the linear response. In both cases, the effects of contrast are substantial over a broad range of spatial frequencies. The effects of contrast on the first-order response (a phase advance at high temporal frequencies, and a relative suppression of low temporal frequency responses) are similar to the amplitude changes and phase changes observed in the second-order frequency response as contrast is varied. Furthermore, the idea that most of the shape change in the second-order frequency response occurs before the static non-linearity suggests that the amplitude changes and phase shifts of the pure second harmonics should be about twice that of the corresponding first-order response changes. This prediction is supported by our data. Therefore we think that the same underlying mechanism is involved in these effects. This hypothesis has significant implications for modelling the functional organization of the retina.

Consequences for retinal organization

We have previously proposed that L_1 in the simple sandwich model might be the bipolar cell (Victor *et al.* 1977). The identification of L_1 with the bipolar cell layer was

advanced on the basis of evidence in other vertebrate retinae that the bipolar responses were approximately linear (Marmarelis & Naka, 1972) and that strong non-linearities first appeared in the amacrine cells (Werblin & Dowling, 1969; Naka, Marmarelis & Chan, 1975). That the effect of contrast on L_1 strongly resembles its effect on the first-order responses of X and Y cells strengthens this identification, for it suggests that the contrast gain control operates before the 'linear' and 'non-linear' pathways diverge.

Previously we have proposed that the network C which generates the contrast signal I_C is the pooled response of the Y cell subunits, since (1) I_C is even order in light intensity, (2) I_C is summed over a wide region, as demonstrated by spatial summation experiments and (3) the spatial and temporal properties of C resemble those of the non-linear subunits (Shapley & Victor, 1979). We are therefore led to the conclusion that this signal, generated by the subunits, is fed back to modulate the behaviour of the front end of the subunits. This feed-back has a natural correlation with the anatomy of the inner plexiform layer in the cat, which possesses numerous amacrine-to-bipolar and amacrine-to-amacrine synapses (Levick, 1975; Kolb, Famiglietti & Nelson, 1976). It is also possible that the interplexiform cells (Boycott *et al.* 1975) may play a role in the contrast gain control, because these cells have considerable lateral spread, and are in a position to relay signals generated by the amacrine cells back to the bipolar cells (Kolb & West, 1977).

This work was supported in part, by grants EY188, EY1428, EY1472 and GM1789 from the U.S. National Institutes of Health. One of us (R.M.S.) was supported by a Career Development Award from the U.S. National Eye Institute.

REFERENCES

Boycott, B. B., Dowling, J. E., Fisher, S. K., Kolb, H. & Laties, A. M. (1975). Interplexiform cells of the mammalian retina and their comparison with catecholamine-containing retinal cells. *Proc. R. Soc.* B **191**, 353–368.

Enroth-Cugell, C. & Robson, J. G. (1966). The contrast sensitivity of retinal ganglion cells of the cat. *J. Physiol.* **187**, 517–552.

Hochstein, S. & Shapley, R. M. (1976*a*). Quantitative analysis of retinal ganglion cell classifications. *J. Physiol.* **262**, 237–264.

Hochstein, S. & Shapley, R. M. (1976*b*). Linear and non-linear spatial subunits in Y cat retinal ganglion cells. *J. Physiol.* **262**, 265–284.

Kolb, H., Famiglietti, E. V. & Nelson, R. (1976). Neural connections in the inner plexiform layer of the cat's retina. In *The Structure of the Eye.* III, ed. Yamada, E. & Mishima, S., pp. 319–332. Tokyo: The Japan Journal of Ophthalmology.

Kolb, H. & West, R. (1977). Synaptic connections of the interplexiform cell in the retina of the cat. *J. Neurol.* **6**, 155–170.

Levick, W. R. (1972). Another tungsten microelectrode. *Med. biol. Engng* **10**, 510–515.

Levick, W. R. (1975). Form and function of cat retinal ganglion cells. *Nature, Lond.* **254**, 659–662.

Marmarelis, P. Z. & Naka, K.-I. (1972). White noise analysis of a neuron chain: an application of the Wiener theory. *Science, N.Y.* **175**, 1276–1278.

Naka, K.-I., Marmarelis, P. Z. & Chan, R. Y. (1975). Morphological and functional identification of catfish retinal nerves. III. Functional identification. *J. Neurophysiol.* **38**, 92–131.

Shapley, R. M. & Rossetto, M. (1976). An electronic visual stimulator. *Behav. Res. Meth. & Instrum.* **8**, 15–20.

Shapley, R. M. & Victor, J. D. (1978). The effect of contrast on the transfer characteristics of retinal ganglion cells. *J. Physiol.* **285**, 275–298.

SHAPLEY, R. M. & VICTOR, J. D. (1979). Non-linear spatial summation and the contrast gain control of cat retinal ganglion cells. *J. Physiol.* **290**, 141–163.

SPEKREIJSE, H., ESTEVEZ, O. & REITS, D. (1977). Visual evoked potentials and the physiological analysis of visual processes in man. In *Visual Evoked Potentials in Man*, ed. DESMEDT, J., pp. 16–89. Oxford: Clarendon Press.

VICTOR, J. D. (1979). The functional organization of the receptive fields of cat X and Y retinal ganglion cells. Thesis, The Rockefeller University, New York.

VICTOR, J. D. & KNIGHT, B. W. (1979). Nonlinear analysis with an arbitrary stimulus ensemble. *Q. appl. Math.* **37**, 113–136.

VICTOR, J. D. & SHAPLEY, R. M. (1979*a*). Receptive field mechanisms of cat X and Y retinal ganglion cells. *J. gen. Physiol.* **74**, 275–298.

VICTOR, J. D. & SHAPLEY, R. M. (1979*b*). The nonlinear pathway of Y ganglion cells in the cat retina. *J. gen. Physiol.* **74**, 671–689.

VICTOR, J. D., SHAPLEY, R. M. & KNIGHT, B. W. (1977). Nonlinear analysis of cat retinal ganglion cells in the frequency domain. *Proc. natn. Acad. Sci. U.S.A.* **74**, 3068–3072.

WERBLIN, F. S. & DOWLING, J. E. (1969). Organization of the retina of the mudpuppy, *Necturus maculosus*. II. Intracellular recording. *J. Neurophysiol.* **32**, 339–355.